

Accretion physics at high X-ray spectral resolution: New frontiers and game-changing science

P. Gandhi,¹ T. Kawamuro,² M. Díaz Trigo,³ J.A. Paice,^{1, 4} P.G. Boorman,^{5, 1} M. Cappi,⁶ C. Done,⁷ A.C. Fabian,⁸ K. Fukumura,⁹ J.A. García,¹⁰ C.L. Greenwell,^{1, 3} M. Guainazzi,¹¹ K. Makishima,^{12, 13, 14} M.S. Tashiro,¹⁵ R. Tomaru,⁷ F. Tombesi,^{16, 17, 18, 19} Y. Ueda²⁰

¹School of Physics & Astronomy, University of Southampton, Highfield, Southampton SO17 1BJ, UK

²Núcleo de Astronomía de la Facultad de Ingeniería, Universidad Diego Portales, Av. Ejército Libertador 441, Santiago, Chile

³European Southern Observatory, Karl-Schwarzschild-Strasse 2, 85748 Garching bei München, Germany

⁴Inter-University Centre for Astronomy & Astrophysics, Pune University, Ganeshkhind, Pune 411007, India

⁵Astronomical Institute of the Czech Academy of Sciences, Boční II 1401, CZ-14100 Prague, Czechia

⁶INAF – OAS Bologna, Astrophysics and Space Science Observatory, Via Gobetti 101, Bologna, Italy

⁷Centre for Extragalactic Astronomy, Department of Physics, University of Durham, South Road, Durham, DH1 3LE, UK

⁸Institute of Astronomy, University of Cambridge, Madingley Road, Cambridge CB3 0HA, UK

⁹Department of Physics and Astronomy, James Madison University, Harrisonburg, VA 22807, USA

¹⁰Cahill Center for Astronomy and Astrophysics, California Institute of Technology, Pasadena, CA 91125, USA

¹¹ESA European Space Research and Technology Centre (ESTEC), Keplerlaan 1, NL-2201 AZ Noordwijk, the Netherlands

¹²Kavli Institute for the Physics and Mathematics of the Universe, 5-1-5 Kashiwa-no-ha, Kashiwa, Chiba 277-8683, Japan

¹³Department of Physics, The University of Tokyo, 7-3-1 Hongo, Bunkyo-ku, Tokyo 113-0033, Japan

¹⁴The Institute of Physical and Chemical Research (RIKEN), 2-1 Hirosawa, Wako, Saitama 351-0198, Japan

¹⁵Department of Physics, Saitama University, 255 Shimo-Okubo, Sakura, Saitama 338-8570

¹⁶Department of Physics, Tor Vergata University of Rome, Via della Ricerca Scientifica 1, I-00133 Rome, Italy

¹⁷INAF - Astronomical Observatory of Rome, Via Frascati 33, I-00078 Monte Porzio Catone (Rome), Italy

¹⁸Department of Astronomy, University of Maryland, College Park, MD 20742, USA

¹⁹NASA/Goddard Space Flight Center, Greenbelt, MD 20771, USA

²⁰Department of Astronomy, Kyoto University, Kyoto 606-8502, Japan

Microcalorimeters have demonstrated success in delivering high spectral resolution, and have paved the path to revolutionary new science possibilities in the coming decade of X-ray astronomy. There are several research areas in compact object science that can only be addressed with energy resolution $\Delta E \lesssim 5$ eV at photon energies of a few keV, corresponding to velocity resolution of \lesssim a few hundred km s^{-1} , to be ushered in by microcalorimeters. Here, we review some of these outstanding questions, focusing on how the research landscape is set to be transformed (i) at the interface between accreting supermassive black holes and their host galaxies, (ii) in unravelling the structures of accretion environments, (iii) in resolving long-standing issues on the origins of energy and matter feedback, and (iv) to test mass-scaled unification of accretion and feedback. The need to learn lessons from *Hitomi* and to make improvements in laboratory atomic data precision as well as plasma modeling are highlighted.

1. Introduction

Cosmic X-ray astronomy turns 60 this year [1]. In this relatively short period, X-ray studies have transformed our view of the hot and energetic side of the

universe. But the field still lacks capabilities that are commonplace in other domains. While astronomers have been splitting optical photons into their respective energies for more than a century using prisms and gratings with effective resolving powers ($E/\Delta E$)

of several thousand and more, similar capabilities still do not exist on X-ray telescopes in orbit.

The above threshold in spectral resolution is important on physical grounds. Much of the gas in the cosmos, in planetary systems, stars, the interstellar medium and some clusters of galaxies, shows characteristic motions of order $\sim 100\text{s km s}^{-1}$ [2, 3]. These motions can only be resolved and mapped if $E/\Delta E > 1,000$. A number of key plasma diagnostics including density, ionisation state, and metallicity, rely on isolating weak and often closely spaced emission lines [4]. This, again, requires adequate spectral finesse. Inflows and outflows around galactic nuclei are also often characterised by relatively mild speeds as they traverse the threshold of the central black hole's gravitational sphere of influence [5].

Detecting and splitting X-ray photons is non-trivial. A typical $\sim 10\text{ keV}$ X-ray photon has a wavelength about a thousand times smaller than an optical one. Detecting these requires exceptionally precise optical surface smoothness, and small incidence-angle focusing optics [6]. Absorption and scattering in the Earth's atmosphere necessitates X-ray telescopes being space-based. X-ray gratings can deliver the requisite spectral resolution needed, but currently only at low energies [7, 8, 9]. Most such X-ray observations are photon-starved, and also unsuited to observations of extended objects in which spatial and velocity information gets mangled.

But cosmic X-ray spectroscopy is about to enter a new era through the use of microcalorimeters. These devices can measure the heat deposited in an absorption layer by individual X-ray photons. When cooled to cryogenic temperatures of $\sim 50\text{ mK}$, the detectors achieve low thermal noise and high energy sensitivity [10, 11]. These demanding requirements make them challenging to operate in space, but we can expect $\frac{E}{\Delta E} \gtrsim 1,000$ for astrophysically important spectral signatures spanning the energy range of $E \sim 5\text{--}10\text{ keV}$ with the upcoming generation of X-ray missions [12, 13]. Being non-dispersive, microcalorimeters optimise high energy resolution together with high quantum efficiency for both point-like and extended cosmic sources.

The *Hitomi* mission already gloriously demonstrated the potential of microcalorimeter science in-orbit, uncovering a surprisingly quiescent intergalactic medium in the Perseus cluster of galaxies through measurements of hot plasma spectral fea-

Table 1. Salient nominal parameters of current and approved high spectral resolution X-ray instruments sensitive at 6–7 keV.

Instrument	Ref.	$R = \frac{E}{\Delta E}$	Area (cm^2)
Chandra HETGS	[8]	165	28
XRISM Resolve	[12]	1,200	210
Athena [†] X-IFU	[17]	2,600	1,300

The Spectral Resolution R and the effective area listed are for the Fe K ($\approx 6\text{--}7\text{ keV}$) energy range. The first-order grating parameters are listed for HETGS. Values of $\Delta E = 5\text{ eV}$ and 2 eV are assumed for Resolve and X-IFU, respectively, as nominal goals. [†]At the time of writing, a redefinition exercise is ongoing, to consider optimised science possibilities with a streamlined mission designated *NewAthena*.

tures with an exquisite precision of 10 km s^{-1} [3]. But the mission had barely begun when it suffered a premature demise [14]. This followed prior ill-fated attempts to place other calorimeters in orbit including *Astro-E* and *XRS/Suzaku* [15, 16]. Paving the road to high spectral resolution X-ray astronomy has proved to be exceptionally arduous. At energies above a few keV, in particular, current grating spectrometers lose sensitivity, and X-ray astronomy has never seen a mission exploit this energy regime at high resolution, other than *Hitomi*. This is set to change with *XRISM*'s launch around 2023 [12] and *Athena* [13] in the early 2030s, optimised for energies $E \sim 0.5\text{--}10\text{ keV}$ and spectral resolution $\frac{E}{\Delta E} \gtrsim 1,000$ at some of the key line transition energies. A few key design parameters for these missions and their respective spectrometers are listed in Table 1, and compared against the current best spectral resolution available with gratings on *Chandra*.

Here, we review the game-changing advances expected with microcalorimeters for accreting compact objects. Accretion of matter is the primary mechanism thought to drive the steady growth of black holes in stellar-mass X-ray binary systems (XRBs) as well as in supermassive black holes in active galactic nuclei (AGN), as opposed to the more convulsive merger-driven growth that we are beginning to probe with gravitational-wave discoveries [18].

There are many unifying aspects to the structure of the accretion zones across the full spectrum of compact object masses. Fig. 1 attempts to illustrate this unification in terms of the physical structures and

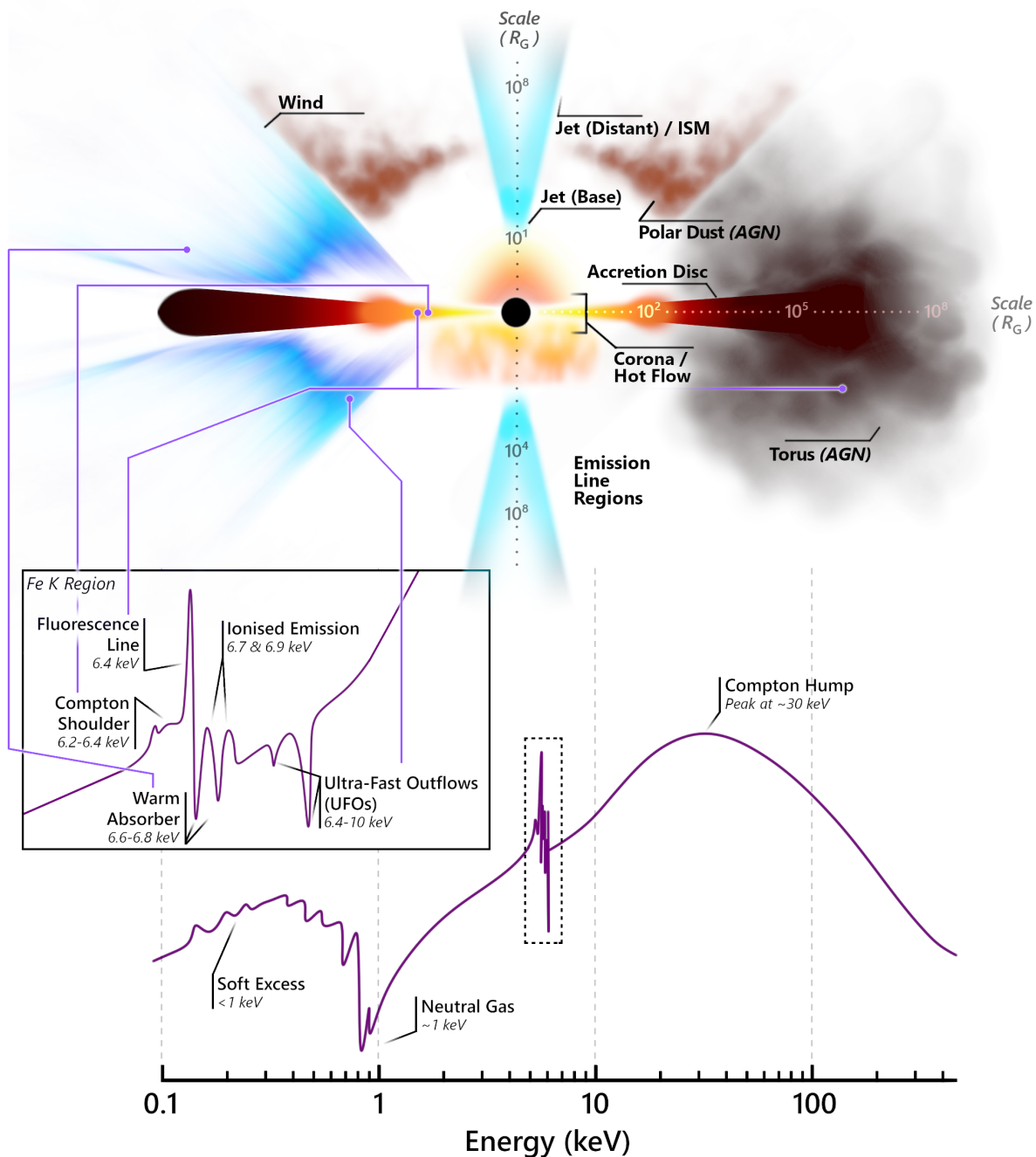


Figure 1. Schematic overview of the environments of accreting compact objects and their X-ray spectra. Many components in the inner accretion regimes are common to both AGN as well as XRBs, including the accretion disc, corona/hot flow, and a relativistic jet. The left vs. the right-hand side depict differing potential models of the outskirts that may be attributed to differing physical conditions (e.g. some components exclusive to AGN are labelled on the right-hand-side). The geometry of several components remains unclear (e.g. the corona is depicted with a spherical vs. an inhomogeneous pancake-like geometry above and below the nucleus, respectively, for illustration) and the origin of others controversial (e.g. ‘the soft excess’). The ‘Emission Line Regions’ indicate the broad and narrow line regions seen in AGN and nebular regions observed in XRBs. Approximate scales are denoted in Gravitational Radii ($R_G = \frac{GM}{c^2}$) extending along the principal axes. The physical components manifest in various spectral signatures depicted at the bottom, and discussed throughout the text. The inset zooms-in on the Iron K energy range around 6–7 keV.

spectral signatures seen across the stellar- and super-massive compact object regimes. In order for a particle to accrete onto a central compact object, it must traverse a huge dynamic range spanning several orders of magnitude in physical scales (and corresponding velocities). If accretion really is scale-invariant, it should be possible to illustrate all compact object environments in terms of approximate mass-scaled size units, as in Fig. 1 where scales are denoted in Gravitational radii ($R_G = \frac{GM}{c^2}$, with G the gravitational constant and c the speed of light).

But not all aspects of such unification attempts are without controversy, as we will discuss herein. Accretion physics at all scales will thus strongly benefit from gains in spectral resolution, in order to resolve these controversies and break new ground in accretion studies. No clean, high quality microcalorimeter spectrum of an accreting source has yet been obtained, so this field is rife with discovery potential, as history has repeatedly demonstrated. Fig. 2 highlights this point by indicating key astronomical discoveries that have been enabled by increasing X-ray spectral resolution and flux sensitivity.

We focus herein on four key questions examining the structures and physical conditions of accreting black hole environments (Section 2), and the nature of energy and matter feedback (Section 3). This should not be read as an exhaustive review, rather a taster of the low-hanging fruit waiting to be plucked in high spectral resolution studies. Space constraints preclude detailed discussions of themes such as the nature of Ultraluminous X-ray sources, tidal disruption events, accreting neutron stars, and investigations of exotic transients.

2. The Accretion Environment

Microcalorimeter science will dramatically widen our reach of the *physical scales* that can be probed around accreting compact objects, as well as the dynamical range of their *physical conditions* amenable to study. We begin by focusing on two key questions encompassing both these aspects:

- [1] How does matter accrete from large scales?
- [2] What are the physical conditions in the inner vicinities around compact objects?

2.1. Gas flows at the interface between the

nucleus and host galaxy: The Keplerian velocity of a particle of interstellar matter located at the radius of influence r of a massive black hole is $v \sim 100\sqrt{(M/10^7 M_\odot)(4\text{pc}/r)} \text{ km s}^{-1}$. Resolving such ‘mild’ velocities requires $E/\Delta E > \text{few } 1,000$. The inability to probe these velocities in X-rays has hampered our understanding of the physical state and kinematics of hot gas at the interface between the black hole and its host galaxy.

Gas needs to shed several orders of magnitude of angular momentum if it is to be accreted from here onto the central engine. The physical mechanisms driving these gas inflows are thought to be gravitational instabilities, triggered either secularly or externally. Secular processes can include bending modes and warps arising in lopsided gas and nuclear stellar discs [27]. On larger scales, stellar bars might bring in fresh supplies of gas from the host galaxy [28]. External processes comprise galactic mergers and interactions, whose role still remains controversial and may be dependent on luminosity and redshift [29, 30]. Microcalorimeters will enable measurements of faint extended gas flows with typical plasma speeds of $\sim 100\text{s km s}^{-1}$ within the hot bulges and haloes of the nearest galaxies.

Gas inflows not only feed, but also obscure the central engine from direct view. The demographics of ‘obscured’ AGN require that nuclear veiling gas must be distributed in a geometrically thick, axisymmetric configuration, generically referred to as the ‘torus’ (Fig. 1). Its presence is key to unifying the characteristics of all AGN under a simple inclination-dependent metric, at least to first-order [31, 32]. In X-rays, the torus manifests as line-of-sight absorption as well as line and continuum scattering signatures, and can explain the integrated shape of the cosmic X-ray background radiation [33, 34, 35]. Yet, its structure and dynamics remain much debated: e.g. is the gas in the toroidal zone undergoing bulk Keplerian rotation, or is it instead dominated by outflows? How is this geometrically thick configuration supported and what is the cloud filling factor [36, 37, 38, 39]?

The canonical torus picture envisions strong reprocessed thermal infrared reemission from obscuring clouds in the *equatorial* plane. Recent interferometric observations have instead revealed a surprisingly different spatial distribution, with dust being found to be elongated along the *polar* direction on scales of a few parsec (Fig. 1), likely driven outwards by radiation

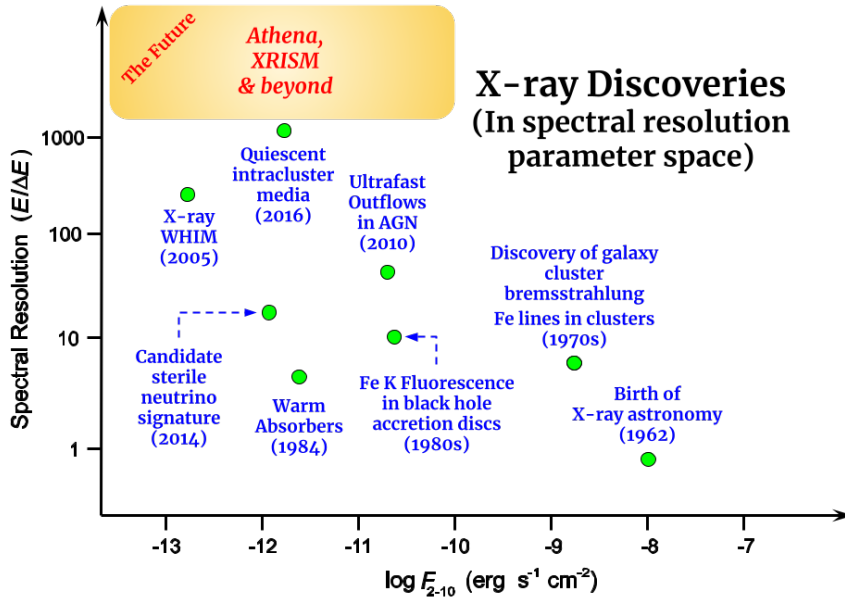


Figure 2. The road to key discoveries in X-ray astronomy as a function of increasing spectral resolution and improving continuum sensitivity, inspired by Harwit [19]. The relevant key discoveries from right to left are from Giacconi et al. [1], Gursky et al. together with Mitchell et al. [20, 21], Barr et al. [22], Tombesi et al. [23], Halpern [24], Hitomi Collaboration [3], Bulbul et al. [25] and, finally, Nicastro et al. [26]. Source fluxes in the 2–10 keV band (or equivalent continuum sensitivities in 100 ksec of exposure) are denoted on the x-axis, and spectral resolution on the y-axis. Unexplored parameter space (at energies $E \geq 6$ keV relevant herein) is indicated by the shaded golden area.

pressure [40]. The dynamical state of cold gas coupled to this dust has been studied with ALMA [41, 42], finding complex flows with characteristic velocities of a few 100 km s^{-1} . The characteristic inmost scale size of the torus as inferred in the infrared is set by radiative physics of dust sublimation [43], but X-ray absorbing gas must span this boundary and exist within the sublimation radius down to scales of the accretion disc. Microcalorimeters will be capable of probing hot gas kinematics spanning the dust sublimation radius.

X-ray microcalorimeters will allow simultaneous studies of the three fundamental phases of interstellar matter – dust, atomic gas, and ionised gas – in particular, high Z -number gaseous elements that ALMA cannot probe. High resolution X-ray spectroscopy offers the capability to decouple these phases, and to track all ionisation states of many high- Z elements, something not possible in other wavebands. With sufficient signal, dust absorption and scattering features could be isolated from gas, delivering estimates of grain size, composition and elemental depletion around the dense environments of accreting sources [44, 45].

The most prominent line transitions in the X-ray regime are associated with Iron (Fe). A relatively high cosmic abundance makes the Fe emission and absorption features excellent spectral probes of gas physical conditions, geometry and dynamics [46, 47], including the torus [48, 49, 50, 51].

Any coherent Keplerian flows should be easily resolved as a result of rotational broadening of the Fe $K\alpha$ and $K\beta$ fluorescence line doublets around 6.4 keV and 7.1 keV, respectively, and the inner edge of the gas torus localised to better than 3% uncertainty in nearby systems (assuming that Keplerian flows at the inner edge dominate the reflected emission [52]).

The only microcalorimeter AGN spectrum obtained so far is that of NGC 1275, the low luminosity nucleus of the Perseus cluster [53], where a narrow Fe line core (with characteristic velocity $v = 500\text{--}1,600 \text{ km s}^{-1}$) was found by *Hitomi*, tracing reflection in a putative extended torus out to scales of a few hundred pc. This single observation is already in conflict with prior (grating) studies of more luminous Seyferts and quasars with *Chandra*, where an Fe $K\alpha$ line width of $v \approx 2,000\text{--}3,000 \text{ km s}^{-1}$, and much broader in some cases, suggested an origin within the torus dust sublimation radius [51, 54, 55, 56]. This could be new evidence of luminosity (or accretion-rate) dependent evolution of the obscuring geometry [57, 58], since NGC 1275 has historically been a weak AGN but with a recent variable, brightening trend [59]. Spatial broadening may also have biased prior grating studies of Seyferts as a result of extended Fe line emission, but the magnitude of this bias remains unclear [60, 56]; spatial extents equivalent to tens to hundreds of pc, orders of magnitude larger than the inner torus, would be required [61].

Microcalorimeter (non-dispersive) spectra of more ‘standard’ AGN, free of contamination by cluster emission, are necessary if we are to scrutinise this putative luminosity dependence and measure gas motions on inner torus scales. Such observations ought to be high priority for *XRISM* and *Athena* upon launch, and can test the hot X-ray gas distribution against the distribution of cooler gas and dust components inferred at other wavelengths in local samples of AGN [62, 63]. Sensitive studies of Fe $K\alpha$ emission on *extended* \sim kpc scales will also become possible in nearby AGN hosts with *Athena*, tracing the reflection echoes of long-term nuclear activity and improving upon photon-starved studies with *Chandra* [64, 65].

Going beyond keplerian flows, high-order grating data from *Chandra* show apparent blueshifts in fluorescent Si emission lines at 1.74 keV of a few hundred km s^{-1} , which may be evidence for outflowing gas in a polar elongated region, an important test of the ‘polar dust scenario’ [66, 51]. But this evidence is still indicative at best, and such studies have been limited to a handful of the brightest, nearby AGN. Sub-mm observations also predominantly find equatorial, as opposed to polar, outflows [42]. X-ray line features from the inner zones of any polar outflow are needed to assess this model critically. The Resolve microcalorimeter on *XRISM* will have a spectral resolution $\frac{E}{\Delta E} \approx 1,200$ at the prominent fluorescence Fe line energy of 6.4 keV, and its low background is expected to robustly uncover outflows down to levels several times fainter than currently possible (Table 1; [67, 68]). *Athena*’s desired combination of high spatial resolution of $\approx 5\text{--}10$ arcsec together with an $\frac{E}{\Delta E} \gtrsim 2,600$ for the X-IFU instrument [17] will greatly expand this science by tracing motions of X-ray reflecting clouds in nearby galactic bulges, and studying the complex interplay between star-formation and AGN activity [69, 42, 13].

The optical depth and ionisation state of obscuring clouds will also be laid bare through the finesse of microcalorimeters. A Compton shoulder (CS) to the neutral Fe line is expected between 6.2–6.4 keV as a result of Compton scattering in cold matter, with a strength determined by gas optical depth and covering factor [70]. *XRISM* is expected to find this feature in many AGN, improving upon a few tentative detections thus far [71, 72], and so provide precise constraints on cloud geometry and optical depth when combined with broadband modelling.

Chemical composition constraints will be possible through accurate metallicity determinations of the Fe edge, and by measuring the the Nickel and Iron fluorescence line strengths relative to each other and to the CS [48]. This will shed light on the origin of the accreting material, e.g. the starburst history in the case of AGN tori [73], or abundances of material that is accreting from the donor star in XRBs [74]. Fe abundance has been found to be super-Solar in the bright Circinus Galaxy ($A_{\text{Fe}} = 1.7$) with $\approx 10\%$ precision [73]. Microcalorimeters will improve upon this, and will cast the net of detection possibilities much wider across the AGN population.

We have discussed probes of kinematic and of gas physical conditions above. Some of the most transformational science is likely to come from the ability to provide simultaneous constraints on these, as we illustrate with the following example. The ionization state of the absorbing and reflecting gas at any distance r from a central engine is quantified by an ‘ionization parameter’ ($\xi = L/nr^2$) dependent on the ionizing power L and the local space density n . For every ionic stage of Iron, the transition energy centroid E ramps up by a few tens of eV (up to Fe XVII, beyond which E increases even faster [75]). This corresponds to $\log \xi$ ramping up approximately by 0.1–0.2 dex at each step [76]. Thus, ξ can be measured in warm plasmas to within a precision of 0.1 dex, if photon energies around the Fe band of $E \sim 6\text{--}7$ keV can be constrained to an accuracy $\lesssim 5\text{--}10$ eV (i.e., a velocity resolution $\Delta v \lesssim 200\text{--}500$ km s^{-1}).

We tested this capability of jointly constraining v and ξ by simulating the presence of a putative (and so-far undetected) ionised outflow in the prototypical Seyfert galaxy NGC 4388. This is amongst the brightest of nearby, hard X-ray Compton-thin (mildly obscured) AGN with a prominent, narrow fluorescence line [77]. Prior studies of this galaxy are used to inform our base X-ray model comprising a power-law and neutral emission line components [78], atop which we introduced an additional putative ionised outflow, with a modest blueshifted velocity $v = -300$ km s^{-1} . The spectrum of the outflow itself is modelled as an ionised reflection component using the XILLVER code [79, 80] with $\log \xi = 1.8$, corresponding to Solar metallicity gas with a volume density of $n_{\text{H}} = 10^6$ cm^{-3} located at a distance of 0.1 pc from a central engine with ionizing luminosity $L \approx 10^{43}$ erg s^{-1} . This could represent the optically-thick base of the dusty polar

outflow known to exist in this source [81]. Its simulated strength has been constrained to be consistent with flux limits inferred from prior X-ray observations [78].

Spectra simulated with 300 ksec-long CCD (*XMM-Newton* EPIC) and microcalorimeter (*XRISM* Resolve) observations are shown in Fig. 3. The simulated CCD emission line is considerably broader than the corresponding line as seen by the microcalorimeter, and is even broader than the plotted energy range. The bottom panel shows the best-fit confidence contours between $\log \xi$ and v , derived by fitting the 6.2–6.6 keV spectral window. Degenerate coupling between the two parameters limits the constraints possible with the CCD, but not for *XRISM*, demonstrating the power of the microcalorimeter to robustly isolate blueshifts from ionisation effects. The structured Fe line complex together with the high spectral resolution of Resolve provide this distinguishing capability. ξ will be constrained to a precision of better than 10%. The uncertainty on v is $\approx 70 \text{ km s}^{-1}$, more than a factor of 20 better than what is possible with CCDs, even in this conservative simulation. Though we have focused on the Fe $K\alpha$ regime here, the $K\alpha$ to $K\beta$ line strengths ratio can also be leveraged to provide further constraints on ξ [52]. *Athena* should improve upon *XRISM*'s best spectral resolution by a further factor of ≈ 2 –4 in the Fe band with its integral field instrument X-IFU [17], allowing additional physical conditions such as abundance studies of the material outflowing from the torus.

As one final line of investigation with no current observational constraints, we mention the unknown prevalence of binary supermassive black holes (SMBHs). Such objects in the process of merging are expected to be prime targets for the next generation of space gravitational wave interferometers [82]. If one or both of the component SMBHs are accreting, complex reflection line profiles are expected [83, 84]. The combination of electromagnetic line shifts with gravitational wave detections will enable unique constraints on relativistic physics and SMBH growth models via accretion. Binary SMBHs that have suffered a recoil of magnitude $\sim 500 \text{ km s}^{-1}$ or more [85] could be easily isolated, if the recoiling SMBH is accreting and shows X-ray line features clearly offset from narrow lines that arise farther out. There is also the potential to learn how nature circumvents

the so-called ‘final parsec problem’ – the unknown mechanism by which binary black holes can lose angular momentum and thereby overcome the final hurdle to merging [86].

2.2. Spectrally resolving the inner accretion

regime: The hottest plasmas at the hearts of accreting sources are key to testing the behaviour of matter under extreme gravity. Their studies open the gateway to measuring several fundamental physical quantities including (1) central object mass M , (2) its spin magnitude a and direction, together with (3) the dynamics and (4) the geometry of the inner accretion regimes. There appear to be some beautifully simple homologies between the stellar-mass and supermassive scales (as illustrated in Fig. 1), though several of these correspondences remain controversial [87]. Studies of both classes of sources are thus enlightening and important.

The inner accretion zones are known to undergo dramatic flux and spectral transitions during well-defined accretion episodes, or ‘outbursts,’ in XRBs. Several distinct transient accretion states have been identified in these outbursts, broadly classified as ‘hard’, ‘soft’ and ‘intermediate’ based upon the X-ray continuum spectral slope, and flux variability amplitude [88, 87]. These are thought to be triggered by instabilities in the accretion flow driven, ultimately, by accretion rate variations in the outer disc [89], though the detailed processes underlying the state transitions, and associated changes in geometry and physical state, remain to be clarified. Longer transition timescales in AGN preclude a proper understanding of accretion states in supermassive black holes. Recent years have seen an increasing number of identifications of so-called ‘changing-look’ or ‘changing-state’ AGN that switch between AGN classes [90]. However, their switchover timescales are far too rapid to be explained solely by viscous accretion rate changes. Irradiation effects, magnetic support, and external perturbations such as tidal disruption events may play a significant role in explaining their rapid transitions [91, 92, 93].

Dynamical motions deep in the gravitational potential wells of compact objects can reach significant relativistic speeds. Low spectral resolution $\frac{E}{\Delta E} \lesssim 100$ thus easily suffices for the most rapid motions, as pioneering studies demonstrated more than 20 years ago

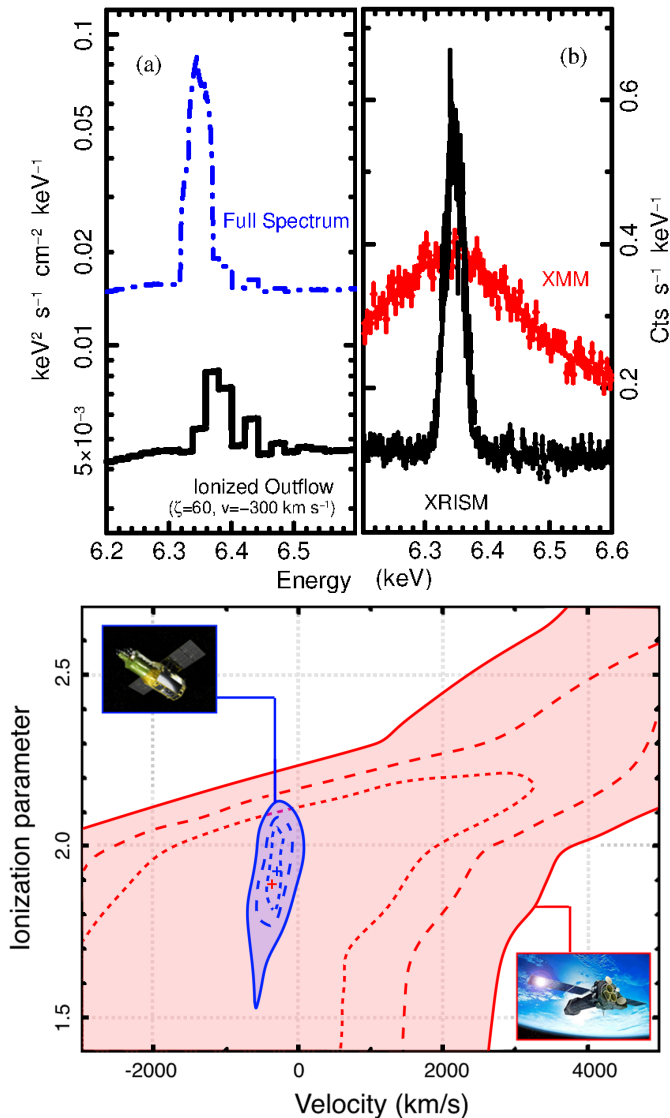


Figure 3. Comparison of joint physical constraints on a mild ionised outflow with a microcalorimeter vs. a CCD. (a): X-ray spectral model of the nearby Seyfert NGC 4388, including an additional ionised outflow in the Fe band. The ionised outflow contributes only a small fraction of the full spectrum line flux. (b): 300 ksec XMM-Newton (CCD; red) and XRISM (microcalorimeter; black) simulated counts spectra. A zoom-in around the Fe lines is shown, while the fit itself has been computed over a wider energy range. Lower panel: Fit contours at 68%, 90%, and 99% confidence levels between the ionization parameter $\log \xi$ and the outflow velocity. The red and blue contours are for XMM-Newton and XRISM, respectively. Negative velocities indicate blueshifts. The Resolve microcalorimeter on XRISM will be sensitive enough to decouple the degeneracy apparent with the CCD, and to pick out fine velocity shifts that are physically relevant in the outer ramparts of the accretion regime.

[94, 95]. Particularly in a disc-dominated accretion state, the inner edge of the disc likely lies close to or reaches the innermost stable circular orbit (ISCO), a key dynamical threshold in the space-time metric of black holes [6]. Inner disc reflection of primary coronal X-ray emission manifests as Fe fluorescence emission broadened due to Doppler and relativistic effects [96]. The magnitude of broadening depends on the relative geometrical configuration and extent of the disc versus the corona and, crucially, scales with a [97, 98]. Because of their ability to constrain the innermost disc zones, broad Fe line studies have matured over the past thirty years and now occupy an important niche within X-ray astronomy [47, 99, 80, 100].

Progress has been impressive enough that the focus has shifted from reducing statistical uncertainties to deliberations on systematic modelling issues. For instance, debates rage regarding the proximity of the inner disc edge to the ISCO in other accretion states [101, 102, 103, 104], and how Fe line constraints match up with those inferred from reverberation mapping and disc continuum modelling techniques [105, 106, 107, 108]. It has also been postulated that it is not the inner disc, but rather the characteristic scale height of the corona, that instead varies with accretion rate [109]. The line strength depends upon the disc inclination angle, and there remain disagreements between the inferred inner disc inclination (as measured in X-rays) vs. the binary orbital plane (as inferred in the optical) [110, 111]. This may point to warped inner disc geometries, which would then need to be accounted for self-consistently when inferring a [112]. The origin of the so-called ‘soft excess’ below 1 keV (Fig. 1) also remains under discussion, with blurred reflection, thermal Comptonisation, and models including contamination due to ionised host galaxy gas having been proffered [113, 114, 115]. Resolving these disagreements has important consequences for cosmic spin measurements, black hole growth, and comparisons between XRBs and for black hole binary mergers events detected by LIGO/Virgo [100, 116]. The relevance of spin in powering relativistic jets also remains controversial [117, 118], partly a consequence of small numbers of accurate spin measurements thus far.

Many of these issues can be traced back to the difficulty of properly decoupling broad reflection and absorption features from the underlying X-ray continuum. The continuum it-

self may also be more complex than a simplistic single thermal plasma, with hybrid plasmas and multi-temperature zones plausibly being more physically realistic [119, 120, 121]. Since most of the radiated accretion power emerges in the X-ray continuum, at least in XRBs, accurately characterising its origin is critical.

If we are to break systematic degeneracies, boosting detected counts alone will not suffice. Higher spectral resolution is critical for proper deconvolution of confusing narrow features, absorption lines, reflection edges and other subtle spectral curvature. As an additional example, Fabian et al. [122] demonstrate the possibility that *absorption* of reflected photons within a disc atmosphere around 8–9 keV can mimic the appearance of a broad blueshifted outflow in the well-studied narrow-line Seyfert 1 galaxy IRAS 13224–3809. If true, this will allow studying not only the disc atmosphere, but also disc dynamics, within a few R_G of the black hole through studies of absorption features. Microcalorimeter spectra could resolve the shape of the absorption feature from the underlying continuum, locating and mapping the disc absorber precisely.

More generally, there is an enormous disparity in the dynamic range of physical scales over which emission and absorption operate. In the deep potential around a rapidly spinning black hole with $a \rightarrow 1$, most of the observed energy release from a luminous disc occurs very close to the centre ($\sim 50\%$ of energy is liberated within $< 5 R_G$; [123]). If this also applies to the coronal emission then it will be similarly compact. By contrast, warm absorption, outflows and dusty gas might arise on disc, torus, or galactic scales, with absorption along many sight-lines that can impact the appearance of that inner emission. Microcalorimeters can make an important contribution in disentangling these. In particular, samples of ‘bare’ AGN, with minimal absorption [124], need to be compared with more complex ones. *XRISM* can place the best constraints on just how bare such AGN are, and how well we can isolate the inner emission to robustly measure spin (e.g. [98]). *Athena*’s high sensitivity will push this envelope to include large ensembles of targets at high redshift. *k*-corrections will redshift key emission and absorption features to lower observed-frame energies where X-IFU’s effective area will peak [17]. For example, mean uncertainties on spin a under conservative assumptions could be < 0.05 [125]. Ideally, this would be further combined with broadband

spectral sensitivity (e.g. with *NuSTAR* [126] or future missions sensitive above ~ 10 keV), in order to accurately model the underlying continuum to high energies. This was highlighted in a recent study of one of the brightest X-ray transients MAXI J1820+070 [127], where a ~ 1 keV blackbody emission-excess has been reported that cannot be explained by disc continuum nor standard Fe fluorescence [128]. Instead, it is interpreted as thermal emission from a non-zero torque arising at the plunge region *inside* the ISCO where matter freely falls into the black hole [128]. Other transients may already have shown this feature [129], but its faintness makes its detection and study non-trivial. Any additional ionised outflows superposed on this would render this near-impossible to isolate and interpret. Coordinated observations with microcalorimeters will thus be crucial to testing this scenario.

Sources that happen to lie edge-on as seen from our vantage point will provide a unique line-of-sight to study the composition of their disc atmospheres. In particular, for those seen at inclinations $\geq 80^\circ$, scattering off extended plasma overlying the disc will dominate, without being blinded by radiation from the central accretion disc. Expected recombination X-ray emission should allow us to probe the plasma metallicity, density and ionisation structure [130]. Pushing down to energy resolutions $\Delta E \lesssim 10$ eV with microcalorimeters will open up the possibility to precisely measure radial stratification within the atmosphere, and also deconvolve double-peaked disc lines, something not possible with gratings. Only a few of these sources are currently known [131], but *XRISM* and then *Athena* will push the flux limits to which these can be detected.

Finally, it should be possible to detect motions of individual structures within the accretion stream (e.g. hot spots in the disc) in ‘real-time,’ if (i) they are bright enough to stand out above the continuum, and if (ii) they display regular Doppler shifts. Tentative detections have previously been reported from Fe K–bright spots located at radial distances of just $\sim 10 R_G$ in AGN; [136]. Higher spectral resolution time-resolved observations will not only uncover secure examples, but also help to constrain the central compact object mass M by modelling of the dynamical line modulation.

Dynamical line modulations could also be employed to obtain mass constraints for XRBs. If the radial velocity modulation of the donor star, or of the

accretor, can be measured as a function of orbital phase, this leads to an estimate of the binary mass function which, together with independent estimates of the inclination angle, constrains the masses of the individual XRB components. This proposed technique relies on detecting narrow absorption features in the disc wind of the accretor [137] or, complementarily, on emission line fluorescence from the surface of the donor star [138]. The radial velocity sensitivity required is $\sim 10 \text{ km s}^{-1}$, depending upon system parameters [139]. This is within reach of microcalorimeters at the bright end, but it is still unclear whether such features can be routinely isolated and whether their point-of-origin within the binary can be constrained well enough to model the mass function. Prior detections of narrow features with *Chandra* are encouraging [140, 135], and if these techniques work, they have the potential to extend mass function measurements to the highly obscured population of XRBs in the Galaxy – objects that have thus far eluded dynamical mass measurements in the optical [139].

3. Energy and Matter Feedback

We next turn attention to the impact of accretion on the galactic-scale environment, a topic of intense interest in compact object physics, galaxy evolution and cosmology. Specifically, the following questions will shape our discussion below:

[1] Are accretion and outflows scale-invariant?

[2] What drives and regulates energy and momentum feedback?

3.1. Scale-invariance: Supermassive black holes at the centres of galaxies impact their host galaxies via radiation and outflows, the latter being in the form of collimated jets or wide-angle winds [141, 5, 142, 143]. Such energy and momentum ‘feedback’ results in a symbiotic coupling of the central SMBH’s growth to that of the host galaxy, as can be appreciated from the following simple energetic argument [144, 145]: the gravitational binding energy of a typical galaxy is approximately $E_{\text{bind}} \sim 10^{60} (M_{\text{gal}}/10^{12} M_{\odot})^2 / (R_{\text{gal}}/30 \text{ kpc})$ erg. This turns out to be comparable to the rest-mass energy associated with a growing SMBH,

$E_{\text{rest}} \sim 10^{60} (f_C/0.01)(M/10^8 M_{\odot})$ erg, if $f_C = 1\%$, that is, 1% of the rest mass energy can be fed back outwards, coupling to matter on galactic scales. Numerical simulations that have implemented simple energy coupling prescriptions between AGN output and circumnuclear gas have, indeed, succeeded in explaining some tight correlations observed between SMBH masses and host bulge properties [146, 147, 148].

However, the processes transporting energy and metals from the nucleus out to interstellar and circumgalactic scales are complex, as is their net effect on the evolutionary history of the host galaxy. Therefore, it remains an open question whether jets or winds exert a larger influence on such evolution. An important limitation in determining the primary feedback channel is our lack of understanding of how jets and winds are launched, and high X-ray spectral resolution is key for advancing our knowledge of winds.

Accretion disc winds are observed both in XRBs and AGN via highly ionised absorption and emission lines in moderate to high-resolution X-ray spectra [149, 150]. In AGN, winds span a wide range of velocities, from $\sim 100 \text{ km s}^{-1}$ in the so-called ‘warm absorbers’ observed mainly in the ultraviolet or soft X-rays [24, 151], and reaching relativistic speeds in ‘Ultra-Fast Outflows (UFOs)’ [152] of which the prototypical example is PDS 456 [153]. UFOs are, therefore, expected to exert significant kinetic feedback, and thus be important for host galaxy evolution, if confirmed to be at the origin of larger (parsec-scale) molecular outflows [152, 154].

In contrast, most XRB warm absorbers do not show significant blueshifts and even winds in iconic black hole XRBs like GRO J1655–40 and GRS 1915+105 show velocities $\lesssim 2000 \text{ km s}^{-1}$ [155, 156, 157, 149] (but see [158, 159] for examples of larger velocities reported in some neutron star XRBs), and consequently, are not expected to contribute significantly to kinetic feedback. But when winds are present, the large masses expelled, of the order of 10^{18} g s^{-1} , [160, 161], are comparable to mass accretion rates in these objects, and could result in depletion of the outer disc and a halt of accretion onto the compact object [162], thus limiting the duty cycle of the XRB and ultimately determining the amount of global feedback.

Here, it is now important to reduce the uncertainties in the mass outflow rates, estimated as $\dot{M}_{\text{outflow}} =$

$\Omega n m_p r^2 v_{\text{out}}$, where m_p is the proton mass and n , r , v_{out} and Ω are the outflow density, launching radius, velocity and solid angle, respectively. For example, the solid angle of the winds remains ill-constrained, but high detection rates in AGN imply that winds must have wide-angled geometries, with solid angles covering at least 30 % of all sight-lines, and more after accounting for observational biases [163, 152]. In XRBs, there are important state dependences, with detections restricted (until recently) to equatorial sightlines in the soft state [161], though this paradigm may now be changing [164].

A major step in the unification of black hole accretion was the discovery of the fundamental plane of black hole activity relating radio and X-ray luminosities across more than six orders of magnitude in mass M [165, 166], and indicating similar accretion and jet launching physics at all scales (cf. Fig. 1). Since winds, similar to jets, are a fundamental piece in the accretion–ejection paradigm, we might expect that they also scale with M .

However, this scaling remains largely unexplored (see [167, 168, 169] for a few attempts), mostly due to the paucity of data and the difficulties of characterising the winds. The breakthrough that the field awaits is a better understanding of the primary drivers of wind launching. Microcalorimeters will tackle this in detail, as we discuss in the following section. Better spectral resolution and sensitivity will allow fair comparisons of stellar- and super-massive systems matched on physically meaningful parameters such as accretion state and the Eddington-scaled accretion rate. This will allow us to determine whether differences observed between the stellar and supermassive scales are due to different wind launching *physics* possibly varying with mass scale M , and to ascertain the impact of the wind physics on feedback.

3.2. The Physics of Launching Outflows: Accretion disc winds can be launched by (1) thermal, (2) magnetic or (3) radiation pressure. Which mechanism or mechanisms dominate(s), and whether XRBs and AGN can be unified in this regard, continues to be debated (e.g. [170, 149, 155, 171, 172, 173]). These mechanisms can leave telltale imprints on various absorption (and emission) lines in the X-ray spectral regime. But characterisation of the winds, and conse-

quently of their origin, is hampered by current X-ray instrumentation, with limited capabilities to resolve line profiles, to disentangle different wind components, to measure small ($< 100 \text{ km s}^{-1}$) line shifts, and to overcome saturation effects associated with high optical depths. Fig. 4 attempts to strip down and capture some of these complex effects at play, in order to illustrate the expected imprints schematically. Importantly, due to these limitations, the density-velocity profile of winds, a key diagnostic of their origin [171], remains to be measured.

Thermal (Compton-heated) and magnetic winds differ in that there is a minimum disc radius at which the former can be launched. Such a radius depends on the Compton temperature, the temperature to which the upper layers of the accretion disc are heated by X-rays from the innermost accretion regions, and this temperature is, in turn, uniquely determined by the illuminating spectrum [174]. Consequently, in thermal winds, we expect a small range of velocities, set by the escape velocity at the launching radius (a few hundred to a few thousand km s^{-1} at radii $\sim 10^6\text{--}10^4 R_G$, typical of XRBs in the soft state).

In contrast, it may be possible to launch magnetic winds from across the entire disc, resulting in high speeds for inner disc lines and broad and asymmetric line profiles overall, reflecting the transverse motions that are unique to such winds [175, 176, 177]. This appears to hold true quite generally, despite a broad variety of predictions for the structure of magnetic winds that depends on the initial (uncertain) magnetic field configuration [178, 179, 180].

As one example of a litmus test between these competing models, Fig. 5 presents a simulation of *XRISM*'s capability, relative to the current best grating spectral resolution with HETGS in the Fe band. Here, an optically thick wind has been simulated for the case of the bright 2005 outburst of the black hole XRB GRO J1655–40, assuming both a thermal-radiative [181] and a magnetic driving model [182], respectively. The *Chandra* grating data obtained for this outburst played an influential role in triggering interest in magnetic wind driving models, but this has remained debated [155, 181]. The simulation zooms in on the Fe XXVI doublet at $\approx 6.97 \text{ keV}$, arising from spin–orbit coupling. The magnetic wind extends over a wide range in radii down to regions very close in to the black hole.

It thus shows the characteristic aforementioned blue asymmetry lacking in the thermal wind which originates farther out. *XRISM* will not only measure the absorbing wind properties, but will also allow the profiles to be modelled with far greater fidelity, in a fraction of the exposure time relative to the gratings [181, 177].

In the absence of additional turbulence, the simulated line doublet can be resolved with microcalorimeters for thermal winds. This doublet offers the advantage of being free from line blends impacting other energies, but only weak constraints derived from observations of bright XRBs with third order *Chandra* gratings are currently available on this feature [183, 171]. While turbulence could add additional scatter, a high degree of turbulence is not expected according to current simulations and, most importantly, isotropic turbulence will not result in asymmetric lines [171] (see Fig. 4, lower panel). Overall, this provides a promising potential pathway for distinguishing the underlying launch mechanism.

This picture can be complicated in the presence of radiation pressure, which may drive winds on its own or in combination with thermal or magnetic pressure [170, 184, 185]. Radiation pressure can manifest in multiple ways, including (i) ‘line driving’ which arises from boosted absorption opacities at resonance line transitions, (ii) and ‘continuum driving’ via Thomson scattering in highly ionised gas (a third scenario of ‘dusty AGN outflows’ was discussed in Section 2). In particular, line radiation pressure can drive very fast winds at relatively low luminosities, though inclusion of relativistic deboosting could reduce the expected velocities [186]. In any case, an important requirement for line driving is that the gas must have a low ionisation state in order to support the line force in the first place [187]. Therefore, ionisation of the gas after it has been accelerated, or some degree of shielding in hot discs, is required in order to explain winds that are simultaneously fast and highly ionised [168, 172, 188]. Continuum radiation pressure is instead expected to be more efficient in launching winds at high Eddington accretion rates via Thomson scattering in fully ionised gas [189], or to aid in launching of thermal winds closer to the compact object [170]. In the end, the difficulty in disentangling the role of radiation pressure lies in the need to infer the illumination to which the gas is exposed despite complex radiative transfer effects [190, 191, 192, 172], and to try and recognise

whether ‘failed winds’ (e.g. [169, 188]) or ‘vertically extended coronae’ [193] provide the necessary shielding for line driving in regions that would otherwise be too hot. However, even in this case, magnetic wind line profiles can be extreme (i.e. wider and more asymmetric), helping to disentangle the roles of radiation and magnetic pressure [191, 192, 172].

Proper characterisation of optically thick regions, with equivalent Hydrogen column densities $> 10^{23}$ – 10^{24} cm⁻², is often impossible due to line saturation (see Fig. 4, upper panel). With microcalorimeters, line saturation (and thus opacity) will be reliably measured and lines in crowded regions of the spectrum will be resolved, allowing multiple wind components to be disentangled. Small redshifts signaling the possible presence of failed winds will be then easily identifiable. Crucially, line profiles will be properly resolved in uncrowded regions of the spectrum, such as the Fe_{XXVI} band. Here, the emission component via scattering in the wind also becomes relevant. This emission component will be broad and centred at the rest wavelength, thus reducing the equivalent width of the blueshifted absorption [194]. A precise characterisation of the full profile of the lines will then constrain the scattering fraction, the wind launching radius, and the solid angle, crucial for measuring the mass outflow rate. Determination of the illumination of parts of the disc/wind shielded from the central source will provide clues on the long-standing mystery of how nature prevents wind over-ionisation.

Obscuring and scattering columns in some sources are known to be exceptionally variable. Classic examples include XRBs that approach high Eddington accretion rates such as V404 Cyg, which showed spectacular spectral variability on a broad range of timescales during outburst [195]. It remains unclear how much of this is intrinsic, or caused by variable gas columns and changes in ionisation degree, or a combination of these. Time-resolved high-resolution spectroscopy of key obscuration diagnostics such as the Compton shoulder and absorption edges, obtained during future bright outbursts, should help to resolve this.

Ultimately, line profiles will likely be more complex in reality than depicted in Fig. 4 due to limitations of current simulations, e.g. in the treatment of radiation transfer for optically thick winds, or the inclusion of scattering. However, detailed simulations for different types of winds in AGN already reveal the extent to which precisely determining saturation, mea-

asuring line profiles, and resolving different wind components with microcalorimeters, together with some prior knowledge of systems such as inclination (well constrained for a majority of XRBs) will help to determine the kinematic structure of accretion disc winds for the first time, and to pinpoint their origin [196].

4. Concluding Remarks

If *Hitomi* unlocked the door to X-ray microcalorimetric studies, *XRISM* is expected to throw this door open wide. The decade of the 2030s should then be ripe for detailed exploration of this new parameter space with the next generation of missions, hopefully improving upon *XRISM*'s spectral resolution by a factor of 2 or more [13, 17]. The studies outlined herein represent only the tip of the iceberg in terms of microcalorimeter advancements expected for accretion studies. Unforeseen and exciting serendipitous discoveries beyond these can be expected whenever new parameter space is opened up [19].

We have focused on science that only high spectral resolution X-ray studies can deliver. But accretion is an inherently broadband phenomenon, and there is no doubt that multiwavelength observations coordinated with microcalorimeters will yield novel constraints on a host of important questions, whether it be the link between winds in various ionisation stages in AGN and XRBs [197, 162], the distribution of dust vs. gas in AGN [63] or the accretion–jet connection on timescales relevant for the inner accretion flows [198], to name just a few outstanding issues. The newly operational *James Webb Space Telescope* is also expected to play a pivotal role in addressing these issues, enabling highly sensitive and high spatial resolution mid-infrared constraints that can be compared to X-ray observations.

But all this will only come to fruition if the instruments operate successfully in space, and if systematic uncertainties (both instrumental and modeling) can be kept under control. At the time of writing, a redefinition exercise to optimise *Athena* science under a new mission designation *NewAthena* is being conducted, where such considerations will be paramount. *Hitomi* data highlighted discrepancies of order 16% between Fe abundance estimates from different atomic databases [199], significantly exceeding statistical errors. A putative 3.5 keV feature in deep observations of galaxy clusters and galactic haloes may be a signature of decaying sterile neutrino dark

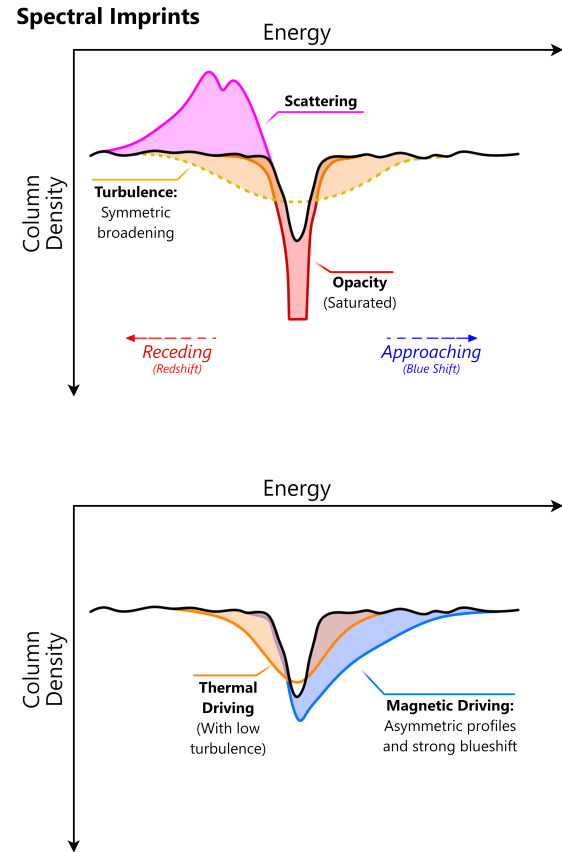


Figure 4. Schematic illustration of the spectral line imprints left by various feedback mechanisms, gas kinematics, and the ambient physical conditions in the accretion system. These influence the position of the line (depicted as Energy on the x-axis), its strength (depicted as a column density on the y-axis), as well as its width. Upper panel: First, we show how line characteristics translate into some generic physical effects. Turbulence results in broadening while a flat bottom denotes line-of-sight optically-thick absorption. Scattering can mimic apparent redshifted emission and P Cygni-like profiles. Line shifts due to approaching and receding motions are indicated. Lower panel: Next, we show profiles expected for isolated lines driven by thermal and magnetic winds. The latter are expected to preferentially show stronger blue skews (based on [176]), though other shapes, including red skews, are possible depending on the detailed photoionisation balance and the wind density at the innermost launching region, [196, 177]. However, the magnetically-driven lines are expected to be significantly more asymmetric than in the case of thermal winds. The spectral resolution of microcalorimeters to be flown aboard *XRISM* and *Athena* is similar to the width of the line expected for thermal driving with low turbulence (or better) in typical Galactic XRBs, so these lines will easily be resolved.

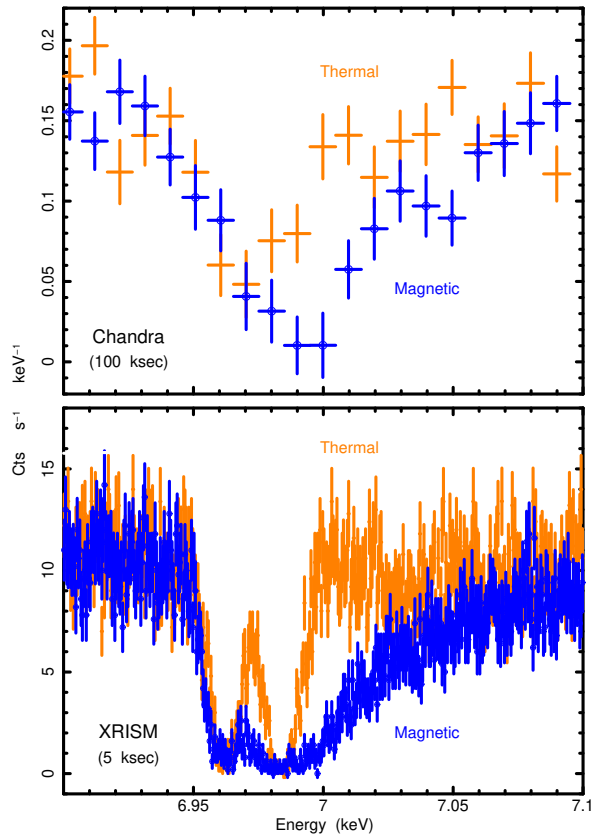


Figure 5. Simulations of XRB thermal vs. magnetic winds. Fe XXVI doublet resulting from thermal (orange points) and magnetic (blue circled points) winds simulated with the parameters of the black hole XRB GRO J1655–40 during its 2005 outburst [182, 181]. The upper/lower panels show simulations of 100 ksec/5 ksec observations with the Chandra gratings and with the XRISM microcalorimeter Resolve, respectively. The Chandra gratings are photon-starved and cannot resolve the doublet. The asymmetry of the line profiles in the magnetic wind is also not unambiguously captured, so that the observations cannot distinguish a magnetic wind from a thermal wind with a high turbulence. XRISM easily overcomes these handicaps, in far shorter an exposure.

matter particles [25]. But this also remains controversial, and ill-appreciated processes such as charge exchange together with abundance mismatches could provide alternative explanations [200, 201]. Hand-in-hand with better modeling and laboratory validation needed to resolve systematic conflicts, adequate resources to support calibration activities will be crucial to ensure optimal science exploitation [202].

5. Author Contributions

The contact authors are MDT, TK and PG, all of whom contributed equally to the main scientific content presented herein. PG led the conception, coordination and thematic definition of this work, together with participants of the XCalibur2019 international workshop at Winchester, UK, in July 2019¹. The focus of the workshop was to identify and review game-changing science to be expected in forthcoming microcalorimeter missions, serving as a genesis for this review. JAP executed the artistic design of the schematic diagram and contributed to the design of all other figures herein. TK is responsible for Section 2 and MDT led Section 3. All authors read and contributed to the overall text.

6. Acknowledgements

We thank two anonymous reviewers for help in improving the content discussion. Dedicated to those who have worked to make microcalorimeter science a reality. Partially supported by the University of Southampton STAG (Theory, Astronomy and Gravity) Research Centre.

References

- [1] Giacconi, R., Gursky, H., Paolini, F. R. & Rossi, B. B. Evidence for x Rays From Sources Outside the Solar System. *Phys. Rev. Lett.* **9**, 439–443 (1962).
- [2] Branduardi-Raymont, G. *et al.* The Hot and Energetic Universe: Solar system and exoplanets. *arXiv e-prints* arXiv:1306.2332 (2013).
- [3] Hitomi Collaboration *et al.* The quiescent intra-cluster medium in the core of the Perseus cluster. *Nature* **535**, 117–121 (2016).

¹<http://www.astro.soton.ac.uk/xcal2019/>

- [4] Hitomi Collaboration *et al.* Solar abundance ratios of the iron-peak elements in the Perseus cluster. *Nature* **551**, 478–480 (2017).
- [5] Fabian, A. C. Observational Evidence of Active Galactic Nuclei Feedback. *Annu. Rev. Astron. Astrophys.* **50**, 455–489 (2012).
- [6] Seward, F. D. & Charles, P. A. *Exploring the X-ray Universe* (Cambridge University Press, ISBN: 9780521884839, 2010).
- [7] Brinkman, A. C. *et al.* First Light Measurements of Capella with the Low-Energy Transmission Grating Spectrometer aboard the Chandra X-Ray Observatory. *Astrophys. J. Lett.* **530**, L111–L114 (2000).
- [8] Canizares, C. R. *et al.* The Chandra High-Energy Transmission Grating: Design, Fabrication, Ground Calibration, and 5 Years in Flight. *PASP* **117**, 1144–1171 (2005).
- [9] den Herder, J. W. *et al.* The Reflection Grating Spectrometer on board XMM-Newton. *Astron. Astrophys.* **365**, L7–L17 (2001).
- [10] Porter, F. S. *et al.* The detector subsystem for the SXS instrument on the ASTRO-H Observatory. In Arnaud, M., Murray, S. S. & Takahashi, T. (eds.) *Space Telescopes and Instrumentation 2010: Ultraviolet to Gamma Ray*, vol. 7732 of *Society of Photo-Optical Instrumentation Engineers (SPIE) Conference Series*, 77323J (2010).
- [11] Mitsuda, K. *et al.* The high-resolution x-ray microcalorimeter spectrometer system for the SXS on ASTRO-H. In Arnaud, M., Murray, S. S. & Takahashi, T. (eds.) *Space Telescopes and Instrumentation 2010: Ultraviolet to Gamma Ray*, vol. 7732 of *Society of Photo-Optical Instrumentation Engineers (SPIE) Conference Series*, 773211 (2010).
- [12] Tashiro, M. *et al.* Concept of the X-ray Astronomy Recovery Mission. In *Space Telescopes and Instrumentation 2018: Ultraviolet to Gamma Ray*, vol. 10699 of *Society of Photo-Optical Instrumentation Engineers (SPIE) Conference Series*, 1069922 (2018).
- [13] Nandra, K. *et al.* The Hot and Energetic Universe: A White Paper presenting the science theme motivating the Athena+ mission. *arXiv e-prints* arXiv:1306.2307 (2013).
- [14] Takahashi, T. *et al.* Hitomi (ASTRO-H) X-ray Astronomy Satellite. *Journal of Astronomical Telescopes, Instruments, and Systems* **4**, 021402 (2018).
- [15] Kelley, R. L. *et al.* The Suzaku High Resolution X-Ray Spectrometer. *PASJ* **59**, 77–112 (2007).
- [16] Gandhi, P. Fourth time's a XARM. *Nature Astronomy* **2**, 434–436 (2018).
- [17] Barret, D. *et al.* The ATHENA X-ray Integral Field Unit (X-IFU). In den Herder, J.-W. A., Nikzad, S. & Nakazawa, K. (eds.) *Space Telescopes and Instrumentation 2018: Ultraviolet to Gamma Ray*, vol. 10699 of *Society of Photo-Optical Instrumentation Engineers (SPIE) Conference Series*, 106991G (2018).
- [18] Abbott, B. P. *et al.* Observation of Gravitational Waves from a Binary Black Hole Merger. *Phys. Rev. Lett.* **116**, 061102 (2016).
- [19] Harwit, M. *Cosmic discovery. The search, scope, and heritage of astronomy* (1981).
- [20] Gursky, H. *et al.* A Strong X-Ray Source in the Coma Cluster Observed by UHURU. *Astrophys. J. Lett.* **167**, L81 (1971).
- [21] Mitchell, R. J., Culhane, J. L., Davison, P. J. N. & Ives, J. C. Ariel 5 observations of the X-ray spectrum of the Perseus cluster. *Mon. Not. R. Astron. Soc.* **175**, 29P–34P (1976).
- [22] Barr, P., White, N. E. & Page, C. G. The discovery of low-level iron K line emission from CYG X-1. *Mon. Not. R. Astron. Soc.* **216**, 65P–70 (1985).
- [23] Tombesi, F. *et al.* Evidence for ultra-fast outflows in radio-quiet AGNs. I. Detection and statistical incidence of Fe K-shell absorption lines. *Astron. Astrophys.* **521**, A57 (2010).
- [24] Halpern, J. P. Variable X-ray absorption in the QSO MR 2251-178. *Astrophys. J.* **281**, 90–94 (1984).

- [25] Bulbul, E. *et al.* Detection of an Unidentified Emission Line in the Stacked X-Ray Spectrum of Galaxy Clusters. *Astrophys. J.* **789**, 13 (2014).
- [26] Nicastro, F. *et al.* The mass of the missing baryons in the X-ray forest of the warm-hot intergalactic medium. *Nature* **433**, 495–498 (2005).
- [27] Hopkins, P. F., Hayward, C. C., Narayanan, D. & Hernquist, L. The origins of active galactic nuclei obscuration: the 'torus' as a dynamical, unstable driver of accretion. *Mon. Not. R. Astron. Soc.* **420**, 320–339 (2012).
- [28] Cisternas, M. *et al.* The Role of Bars in AGN Fueling in Disk Galaxies Over the Last Seven Billion Years. *Astrophys. J.* **802**, 137 (2015).
- [29] Marian, V. *et al.* Major Mergers Are Not the Dominant Trigger for High-accretion AGNs at $z \sim 2$. *Astrophys. J.* **882**, 141 (2019).
- [30] Storchi-Bergmann, T. & Schnorr-Müller, A. Observational constraints on the feeding of supermassive black holes. *Nature Astronomy* **3**, 48–61 (2019).
- [31] Antonucci, R. Unified models for active galactic nuclei and quasars. *Annu. Rev. Astron. Astrophys.* **31**, 473–521 (1993).
- [32] Netzer, H. Revisiting the Unified Model of Active Galactic Nuclei. *Annu. Rev. Astron. Astrophys.* **53**, 365–408 (2015).
- [33] Gilli, R., Comastri, A. & Hasinger, G. The synthesis of the cosmic X-ray background in the Chandra and XMM-Newton era. *Astron. Astrophys.* **463**, 79–96 (2007).
- [34] Ueda, Y., Akiyama, M., Hasinger, G., Miyaji, T. & Watson, M. G. Toward the Standard Population Synthesis Model of the X-Ray Background: Evolution of X-Ray Luminosity and Absorption Functions of Active Galactic Nuclei Including Compton-thick Populations. *Astrophys. J.* **786**, 104 (2014).
- [35] Ananna, T. T. *et al.* The Accretion History of AGNs. I. Supermassive Black Hole Population Synthesis Model. *Astrophys. J.* **871**, 240 (2019).
- [36] Elvis, M. A Structure for Quasars. *Astrophys. J.* **545**, 63–76 (2000).
- [37] Markowitz, A. G., Krumpe, M. & Nikutta, R. First X-ray-based statistical tests for clumpy-torus models: eclipse events from 230 years of monitoring of Seyfert AGN. *Mon. Not. R. Astron. Soc.* **439**, 1403–1458 (2014).
- [38] Hopkins, P. F., Torrey, P., Faucher-Giguère, C.-A., Quataert, E. & Murray, N. Stellar and quasar feedback in concert: effects on AGN accretion, obscuration, and outflows. *Mon. Not. R. Astron. Soc.* **458**, 816–831 (2016).
- [39] Ramos Almeida, C. & Ricci, C. Nuclear obscuration in active galactic nuclei. *Nature Astronomy* **1**, 679–689 (2017).
- [40] Hönig, S. F. *et al.* Dust in the Polar Region as a Major Contributor to the Infrared Emission of Active Galactic Nuclei. *Astrophys. J.* **771**, 87 (2013).
- [41] Izumi, T., Wada, K., Fukushige, R., Hamamura, S. & Kohno, K. Circumnuclear Multiphase Gas in the Circinus Galaxy. II. The Molecular and Atomic Obscuring Structures Revealed with ALMA. *Astrophys. J.* **867**, 48 (2018).
- [42] García-Burillo, S. *et al.* The Galaxy Activity, Torus, and Outflow Survey (GATOS). I. ALMA images of dusty molecular tori in Seyfert galaxies. *Astron. Astrophys.* **652**, A98 (2021).
- [43] Barvainis, R. Hot dust and the near-infrared bump in the continuum spectra of quasars and active galactic nuclei. *Astrophys. J.* **320**, 537–544 (1987).
- [44] Rogantini, D. *et al.* Investigating the interstellar dust through the Fe K-edge. *Astron. Astrophys.* **609**, A22 (2018).
- [45] Corrales, L. R., García, J., Wilms, J. & Baganoff, F. The dust-scattering component of X-ray extinction: effects on continuum fitting and high-resolution absorption edge structure. *Mon. Not. R. Astron. Soc.* **458**, 1345–1351 (2016).

- [46] Basko, M. M. K-fluorescence lines in spectra of X-ray binaries. *Astrophys. J.* **223**, 268–281 (1978).
- [47] Fabian, A. C., Iwasawa, K., Reynolds, C. S. & Young, A. J. Broad Iron Lines in Active Galactic Nuclei. *PASP* **112**, 1145–1161 (2000).
- [48] Molendi, S., Bianchi, S. & Matt, G. Iron and nickel line properties in the X-ray-reflecting region of the Circinus galaxy. *Mon. Not. R. Astron. Soc.* **343**, L1–L4 (2003).
- [49] Murphy, K. D. & Yaqoob, T. An X-ray spectral model for Compton-thick toroidal reproducers. *Mon. Not. R. Astron. Soc.* **397**, 1549–1562 (2009).
- [50] Baloković, M. *et al.* New Spectral Model for Constraining Torus Covering Factors from Broadband X-Ray Spectra of Active Galactic Nuclei. *Astrophys. J.* **854**, 42 (2018).
- [51] Shu, X. W., Yaqoob, T. & Wang, J. X. The Cores of the Fe $K\alpha$ Lines in Active Galactic Nuclei: An Extended Chandra High Energy Grating Sample. *Astrophys. J. Suppl.* **187**, 581–606 (2010).
- [52] Reynolds, C. *et al.* ASTRO-H White Paper - AGN Reflection. *arXiv e-prints* arXiv:1412.1177 (2014).
- [53] Hitomi Collaboration *et al.* Hitomi observation of radio galaxy NGC 1275: The first X-ray microcalorimeter spectroscopy of Fe- $K\alpha$ line emission from an active galactic nucleus. *PASJ* **70**, 13 (2018).
- [54] Minezaki, T. & Matsushita, K. A New Black Hole Mass Estimate for Obscured Active Galactic Nuclei. *Astrophys. J.* **802**, 98 (2015).
- [55] Gandhi, P., Hönig, S. F. & Kishimoto, M. The Dust Sublimation Radius as an Outer Envelope to the Bulk of the Narrow Fe $K\alpha$ Line Emission in Type 1 AGNs. *Astrophys. J.* **812**, 113 (2015).
- [56] Uematsu, R. *et al.* X-Ray Constraint on the Location of the AGN Torus in the Circinus Galaxy. *Astrophys. J.* **913**, 17 (2021).
- [57] Ezhikode, S. H. *et al.* Determining the torus covering factors for a sample of type 1 AGN in the local Universe. *Mon. Not. R. Astron. Soc.* **472**, 3492–3511 (2017).
- [58] Ricci, C. *et al.* The close environments of accreting massive black holes are shaped by radiative feedback. *Nature* **549**, 488–491 (2017).
- [59] Fabian, A. C., Walker, S. A., Pinto, C., Russell, H. R. & Edge, A. C. Effects of the variability of the nucleus of NGC 1275 on X-ray observations of the surrounding intracluster medium. *Mon. Not. R. Astron. Soc.* **451**, 3061–3067 (2015).
- [60] Liu, J. The intrinsic line width of the Fe $K\alpha$ line of AGN. *Mon. Not. R. Astron. Soc.* **463**, L108–L111 (2016).
- [61] Masterson, M. & Reynolds, C. S. Probing the Extent of Fe $K\alpha$ Emission in Nearby Active Galactic Nuclei Using Multi-order Analysis of Chandra High Energy Transmission Grating Data. *Astrophys. J.* **936**, 66 (2022).
- [62] Alonso-Herrero, A. *et al.* The Galaxy Activity, Torus, and Outflow Survey (GATOS). II. Torus and polar dust emission in nearby Seyfert galaxies. *Astron. Astrophys.* **652**, A99 (2021).
- [63] Esparza-Arredondo, D. *et al.* The dust-gas AGN torus as constrained from X-ray and mid-infrared observations. *Astron. Astrophys.* **651**, A91 (2021).
- [64] Marinucci, A. *et al.* The X-ray reflector in NGC 4945: a time- and space-resolved portrait. *Mon. Not. R. Astron. Soc.* **423**, L6–L10 (2012).
- [65] Andonie, C. *et al.* Localizing narrow Fe $K\alpha$ emission within bright AGN. *Astron. Astrophys.* **664**, A46 (2022).
- [66] Liu, J., Hönig, S. F., Ricci, C. & Paltani, S. X-ray signatures of the polar dusty gas in AGN. *Mon. Not. R. Astron. Soc.* **490**, 4344–4352 (2019).
- [67] Guainazzi, M. & Tashiro, M. S. The Hot Universe with XRISM and Athena. In Asada, K., de

- Gouveia Dal Pino, E., Giroletti, M., Nagai, H. & Nemmen, R. (eds.) *Perseus in Sicily: From Black Hole to Cluster Outskirts*, vol. 342, 29–36 (2020).
- [68] XRISM Science Team. Science with the X-ray Imaging and Spectroscopy Mission (XRISM) arXiv:2003.04962 (2020).
- [69] Kawamuro, T., Izumi, T. & Imanishi, M. A Chandra and ALMA study of X-ray-irradiated gas in the central ~ 100 pc of the Circinus galaxy. *PASJ* **71**, 68 (2019).
- [70] Matt, G. The iron $K\alpha$ Compton shoulder in transmitted and reflected spectra. *Mon. Not. R. Astron. Soc.* **337**, 147–150 (2002).
- [71] Iwasawa, K., Fabian, A. C. & Matt, G. The iron K line complex in NGC1068: implications for X-ray reflection in the nucleus. *Mon. Not. R. Astron. Soc.* **289**, 443–449 (1997).
- [72] Bianchi, S. *et al.* Flux and spectral variations in the Circinus Galaxy. *Astron. Astrophys.* **396**, 793–799 (2002).
- [73] Hikitani, M., Ohno, M., Fukazawa, Y., Kawaguchi, T. & Odaka, H. Compton Shoulder Diagnostics in Active Galactic Nuclei for Probing the Metallicity of the Obscuring Compton-thick Tori. *Astrophys. J.* **867**, 80 (2018).
- [74] Watanabe, S. *et al.* Detection of a Fully Resolved Compton Shoulder of the Iron $K\alpha$ Line in the Chandra X-Ray Spectrum of GX 301-2. *Astrophys. J. Lett.* **597**, L37–L40 (2003).
- [75] Kallman, T. R. & McCray, R. X-ray nebular models. *Astrophys. J. Suppl.* **50**, 263–317 (1982).
- [76] Nagase, F. Accretion-powered X-ray pulsars. *PASJ* **41**, 1 (1989).
- [77] Oh, K. *et al.* The 105-Month Swift-BAT All-sky Hard X-Ray Survey. *Astrophys. J. Suppl.* **235**, 4 (2018).
- [78] Shirai, H. *et al.* Detailed Hard X-Ray Measurements of Nuclear Emission from the Seyfert2 Galaxy NGC4388 with Suzaku. *PASJ* **60**, S263 (2008).
- [79] Dauser, T., Garcia, J., Parker, M. L., Fabian, A. C. & Wilms, J. The role of the reflection fraction in constraining black hole spin. *Mon. Not. R. Astron. Soc.* **444**, L100–L104 (2014).
- [80] García, J. *et al.* Improved Reflection Models of Black Hole Accretion Disks: Treating the Angular Distribution of X-Rays. *Astrophys. J.* **782**, 76 (2014).
- [81] Asmus, D., Hönig, S. F. & Gandhi, P. The Subarcsecond Mid-infrared View of Local Active Galactic Nuclei. III. Polar Dust Emission. *Astrophys. J.* **822**, 109 (2016).
- [82] Hughes, S. A. Untangling the merger history of massive black holes with LISA. *Mon. Not. R. Astron. Soc.* **331**, 805–816 (2002).
- [83] Yu, Q. & Lu, Y. Fe $K\alpha$ line: A tool to probe massive binary black holes in Active Galactic Nuclei? *Astron. Astrophys.* **377**, 17–22 (2001).
- [84] Jovanović, P., Borka Jovanović, V., Borka, D. & Popović, L. Č. Possible observational signatures of supermassive black hole binaries in their Fe $K\alpha$ line profiles. *Contributions of the Astronomical Observatory Skalnaté Pleso* **50**, 219–234 (2020).
- [85] Komossa, S., Zhou, H. & Lu, H. A Recoiling Supermassive Black Hole in the Quasar SDSS J092712.65+294344.0? *Astrophys. J. Lett.* **678**, L81 (2008).
- [86] Armitage, P. J. & Natarajan, P. Accretion during the Merger of Supermassive Black Holes. *Astrophys. J. Lett.* **567**, L9–L12 (2002).
- [87] Done, C., Gierliński, M. & Kubota, A. Modelling the behaviour of accretion flows in X-ray binaries. Everything you always wanted to know about accretion but were afraid to ask. *Astron. Astrophys. Rev.* **15**, 1–66 (2007).
- [88] Remillard, R. A. & McClintock, J. E. X-Ray Properties of Black-Hole Binaries. *Annu. Rev. Astron. Astrophys.* **44**, 49–92 (2006).

- [89] Lasota, J.-P. The disc instability model of dwarf novae and low-mass X-ray binary transients. *New Astron. Rev.* **45**, 449–508 (2001).
- [90] Shappee, B. J. *et al.* The Man behind the Curtain: X-Rays Drive the UV through NIR Variability in the 2013 Active Galactic Nucleus Outburst in NGC 2617. *Astrophys. J.* **788**, 48 (2014).
- [91] MacLeod, C. L. *et al.* A systematic search for changing-look quasars in SDSS. *Mon. Not. R. Astron. Soc.* **457**, 389–404 (2016).
- [92] Dexter, J. & Begelman, M. C. Extreme AGN variability: evidence of magnetically elevated accretion? *Mon. Not. R. Astron. Soc.* **483**, L17–L21 (2019).
- [93] Ricci, C. *et al.* The Destruction and Recreation of the X-Ray Corona in a Changing-look Active Galactic Nucleus. *Astrophys. J. Lett.* **898**, L1 (2020).
- [94] Fabian, A. C., Rees, M. J., Stella, L. & White, N. E. X-ray fluorescence from the inner disc in Cygnus X-1. *Mon. Not. R. Astron. Soc.* **238**, 729–736 (1989).
- [95] Tanaka, Y. *et al.* Gravitationally redshifted emission implying an accretion disk and massive black hole in the active galaxy MCG-6-30-15. *Nature* **375**, 659–661 (1995).
- [96] George, I. M. & Fabian, A. C. X-ray reflection from cold matter in Active Galactic Nuclei and X-ray binaries. *Mon. Not. R. Astron. Soc.* **249**, 352 (1991).
- [97] Laor, A. Line Profiles from a Disk around a Rotating Black Hole. *Astrophys. J.* **376**, 90 (1991).
- [98] Brenneman, L. *Measuring the Angular Momentum of Supermassive Black Holes* (Measuring the Angular Momentum of Supermassive Black Holes, Springer Briefs in Astronomy, ISBN 978-1-4614-7770-9, 2013).
- [99] Dovčiak, M., Karas, V. & Yaqoob, T. An Extended Scheme for Fitting X-Ray Data with Accretion Disk Spectra in the Strong Gravity Regime. *Astrophys. J. Suppl.* **153**, 205–221 (2004).
- [100] Reynolds, C. S. Observational Constraints on Black Hole Spin. *Annu. Rev. Astron. Astrophys.* **59**, 117–154 (2021).
- [101] Miller, J. M., Homan, J. & Miniutti, G. A Prominent Accretion Disk in the Low-Hard State of the Black Hole Candidate SWIFT J1753.5-0127. *Astrophys. J. Lett.* **652**, L113–L116 (2006).
- [102] Done, C. & Diaz Trigo, M. A re-analysis of the iron line in the XMM-Newton data from the low/hard state in GX339-4. *Mon. Not. R. Astron. Soc.* **407**, 2287–2296 (2010).
- [103] Turner, T. J. & Miller, L. X-ray absorption and reflection in active galactic nuclei. *Astron. Astrophys. Rev.* **17**, 47–104 (2009).
- [104] Hagino, K. *et al.* A disc wind interpretation of the strong Fe $K\alpha$ features in 1H 0707-495. *Mon. Not. R. Astron. Soc.* **461**, 3954–3963 (2016).
- [105] McClintock, J. E. *et al.* The Spin of the Near-Extreme Kerr Black Hole GRS 1915+105. *Astrophys. J.* **652**, 518–539 (2006).
- [106] Yamada, S. *et al.* Is the Black Hole in GX 339-4 Really Spinning Rapidly? *Astrophys. J. Lett.* **707**, L109–L113 (2009).
- [107] Uttley, P., Cackett, E. M., Fabian, A. C., Kara, E. & Wilkins, D. R. X-ray reverberation around accreting black holes. *Astron. Astrophys. Rev.* **22**, 72 (2014).
- [108] De Marco, B. *et al.* The inner flow geometry in MAXI J1820+070 during hard and hard-intermediate states. *Astron. Astrophys.* **654**, A14 (2021).
- [109] Kara, E. *et al.* The corona contracts in a black-hole transient. *Nature* **565**, 198–201 (2019).
- [110] Connors, R. M. T. *et al.* Conflicting Disk Inclination Estimates for the Black Hole X-Ray Binary XTE J1550-564. *Astrophys. J.* **882**, 179 (2019).

- [111] Draghis, P. A. *et al.* The Spin and Orientation of the Black Hole in XTE J1908+094. *arXiv:2107.02810* arXiv:2107.02810 (2021).
- [112] Abarr, Q. & Krawczynski, H. The Iron Line Profile from Warped Black Hole Accretion Disks. *Astrophys. J.* **906**, 28 (2021).
- [113] Crummy, J., Fabian, A. C., Gallo, L. & Ross, R. R. An explanation for the soft X-ray excess in active galactic nuclei. *Mon. Not. R. Astron. Soc.* **365**, 1067–1081 (2006).
- [114] Noda, H. *et al.* The Nature of Stable Soft X-Ray Emissions in Several Types of Active Galactic Nuclei Observed by Suzaku. *PASJ* **65**, 4 (2013).
- [115] Petrucci, P. O. *et al.* Testing warm Comptonization models for the origin of the soft X-ray excess in AGNs. *Astron. Astrophys.* **611**, A59 (2018).
- [116] Belczynski, K., Done, C. & Lasota, J. P. All Apples: Comparing black holes in X-ray binaries and gravitational-wave sources. *arXiv e-prints* arXiv:2111.09401 (2021).
- [117] Narayan, R. & McClintock, J. E. Observational evidence for a correlation between jet power and black hole spin. *Mon. Not. R. Astron. Soc.* **419**, L69–L73 (2012).
- [118] Russell, D. M., Gallo, E. & Fender, R. P. Observational constraints on the powering mechanism of transient relativistic jets. *Mon. Not. R. Astron. Soc.* **431**, 405–414 (2013).
- [119] Coppi, P. S. The Physics of Hybrid Thermal/Non-Thermal Plasmas. In Poutanen, J. & Svensson, R. (eds.) *High Energy Processes in Accreting Black Holes*, vol. 161 of *Astronomical Society of the Pacific Conference Series*, 375 (1999).
- [120] Makishima, K. *et al.* Suzaku Results on Cygnus X-1 in the Low/Hard State. *PASJ* **60**, 585 (2008).
- [121] Yamada, S. *et al.* Evidence for a Cool Disk and Inhomogeneous Coronae from Wide-Band Temporal Spectroscopy of Cygnus X-1 with Suzaku. *PASJ* **65**, 80 (2013).
- [122] Fabian, A. C. *et al.* Blueshifted absorption lines from X-ray reflection in IRAS 13224-3809. *Mon. Not. R. Astron. Soc.* **493**, 2518–2522 (2020).
- [123] Thorne, K. S. Disk-Accretion onto a Black Hole. II. Evolution of the Hole. *Astrophys. J.* **191**, 507–520 (1974).
- [124] Walton, D. J., Nardini, E., Fabian, A. C., Gallo, L. C. & Reis, R. C. Suzaku observations of ‘bare’ active galactic nuclei. *Mon. Not. R. Astron. Soc.* **428**, 2901–2920 (2013).
- [125] Barret, D. & Cappi, M. Inferring black hole spins and probing accretion/ejection flows in AGNs with the Athena X-ray Integral Field Unit. *Astron. Astrophys.* **628**, A5 (2019).
- [126] Harrison, F. A. *et al.* The Nuclear Spectroscopic Telescope Array (NuSTAR) High-energy X-Ray Mission. *Astrophys. J.* **770**, 103 (2013).
- [127] Kawamuro, T. *et al.* MAXI/GSC detection of a probable new X-ray transient MAXI J1820+070. *The Astronomer’s Telegram* **11399**, 1 (2018).
- [128] Fabian, A. C. *et al.* The soft state of the black hole transient source MAXI J1820+070: emission from the edge of the plunge region? *Mon. Not. R. Astron. Soc.* **493**, 5389–5396 (2020).
- [129] Oda, S. *et al.* X-ray and optical observations of the black hole candidate MAXI J1828-249. *PASJ* **71**, 108 (2019).
- [130] Jimenez-Garate, M. A., Raymond, J. C. & Liedahl, D. A. The Structure and X-Ray Recombination Emission of a Centrally Illuminated Accretion Disk Atmosphere and Corona. *Astrophys. J.* **581**, 1297–1327 (2002).
- [131] Done, C. *et al.* ASTRO-H White Paper - Low-mass X-ray Binaries. *arXiv e-prints* arXiv:1412.1164 (2014).
- [132] Garcia, J. A. *et al.* Relativistic X-ray Reflection Models for Accreting Neutron Stars. *arXiv e-prints* arXiv:2111.12838 (2021).
- [133] Degenaar, N. *et al.* High-resolution X-Ray Spectroscopy of the Bursting Pulsar GRO J1744-28. *Astrophys. J. Lett.* **796**, L9 (2014).

- [134] Watanabe, S. *et al.* X-Ray Spectral Study of the Photoionized Stellar Wind in Vela X-1. *Astrophys. J.* **651**, 421–437 (2006).
- [135] Torrejón, J. M., Schulz, N. S., Nowak, M. A. & Kallman, T. R. A Chandra Survey of Fluorescence Fe Lines in X-ray Binaries at High Resolution. *Astrophys. J.* **715**, 947–958 (2010).
- [136] Iwasawa, K., Miniutti, G. & Fabian, A. C. Flux and energy modulation of redshifted iron emission in NGC 3516: implications for the black hole mass. *Mon. Not. R. Astron. Soc.* **355**, 1073–1079 (2004).
- [137] Zhang, S.-N., Liao, J. & Yao, Y. Measuring the black hole masses in accreting X-ray binaries by detecting the Doppler orbital motion of their accretion disc wind absorption lines. *Mon. Not. R. Astron. Soc.* **421**, 3550–3556 (2012).
- [138] Dashwood-Brown *et al.*, C. Measuring interacting binary mass functions with X-ray fluorescence. *Mon. Not. R. Astron. Soc. in press* (2022).
- [139] Casares, J. & Jonker, P. G. Mass Measurements of Stellar and Intermediate-Mass Black Holes. *SSRv* **183**, 223–252 (2014).
- [140] Ponti, G., Bianchi, S., Muñoz-Darias, T. & Nandra, K. Measuring masses in low mass X-ray binaries via X-ray spectroscopy: the case of MXB 1659-298. *Mon. Not. R. Astron. Soc.* **481**, L94–L99 (2018).
- [141] McNamara, B. R. & Nulsen, P. E. J. Heating Hot Atmospheres with Active Galactic Nuclei. *Annu. Rev. Astron. Astrophys.* **45**, 117–175 (2007).
- [142] Harrison, C. M. Impact of supermassive black hole growth on star formation. *Nature Astronomy* **1**, 0165 (2017).
- [143] Morganti, R. The many routes to AGN feedback. *Frontiers in Astronomy and Space Sciences* **4**, 42 (2017).
- [144] Silk, J. & Rees, M. J. Quasars and galaxy formation. *Astron. Astrophys.* **331**, L1–L4 (1998).
- [145] Fabian, A. C. The obscured growth of massive black holes. *Mon. Not. R. Astron. Soc.* **308**, L39–L43 (1999).
- [146] Ferrarese, L. & Merritt, D. A Fundamental Relation between Supermassive Black Holes and Their Host Galaxies. *Astrophys. J. Lett.* **539**, L9–L12 (2000).
- [147] Marconi, A. & Hunt, L. K. The Relation between Black Hole Mass, Bulge Mass, and Near-Infrared Luminosity. *Astrophys. J. Lett.* **589**, L21–L24 (2003).
- [148] Di Matteo, T., Springel, V. & Hernquist, L. Energy input from quasars regulates the growth and activity of black holes and their host galaxies. *Nature* **433**, 604–607 (2005).
- [149] Díaz Trigo, M. & Boirin, L. Accretion disc atmospheres and winds in low-mass X-ray binaries. *Astronomische Nachrichten* **337**, 368 (2016).
- [150] Tombesi, F. Accretion disk winds in active galactic nuclei: X-ray observations, models, and feedback. *Astronomische Nachrichten* **337**, 410 (2016).
- [151] Blustin, A. J., Page, M. J., Fuerst, S. V., Branduardi-Raymont, G. & Ashton, C. E. The nature and origin of Seyfert warm absorbers. *Astron. Astrophys.* **431**, 111–125 (2005).
- [152] Tombesi, F. *et al.* Unification of X-ray winds in Seyfert galaxies: from ultra-fast outflows to warm absorbers. *Mon. Not. R. Astron. Soc.* **430**, 1102–1117 (2013).
- [153] Reeves, J. N. *et al.* A Compton-thick Wind in the High-luminosity Quasar, PDS 456. *Astrophys. J.* **701**, 493–507 (2009).
- [154] Feruglio, C. *et al.* The multi-phase winds of Markarian 231: from the hot, nuclear, ultra-fast wind to the galaxy-scale, molecular outflow. *Astron. Astrophys.* **583**, A99 (2015).

- [155] Miller, J. M. *et al.* The magnetic nature of disk accretion onto black holes. *Nature* **441**, 953–955 (2006).
- [156] Ueda, Y., Yamaoka, K. & Remillard, R. GRS 1915+105 in “Soft State”: Nature of Accretion Disk Wind and Origin of X-ray Emission. *Astrophys. J.* **695**, 888–899 (2009).
- [157] Neilsen, J., Petschek, A. J. & Lee, J. C. Accretion disc wind variability in the states of the microquasar GRS 1915+105. *Mon. Not. R. Astron. Soc.* **421**, 502–511 (2012).
- [158] Degenaar, N. *et al.* High-resolution X-Ray Spectroscopy of the Bursting Pulsar GRO J1744-28. *Astrophys. J. Lett.* **796**, L9 (2014).
- [159] Nowak, M. A. *et al.* Chandra-HETGS Characterization of an Outflowing Wind in the Accreting Millisecond Pulsar IGR J17591-2342. *Astrophys. J.* **874**, 69 (2019).
- [160] Ueda, Y., Murakami, H., Yamaoka, K., Dotani, T. & Ebisawa, K. Chandra High-Resolution Spectroscopy of the Absorption-Line Features in the Low-Mass X-Ray Binary GX 13+1. *Astrophys. J.* **609**, 325–334 (2004).
- [161] Ponti, G. *et al.* Ubiquitous equatorial accretion disc winds in black hole soft states. *Mon. Not. R. Astron. Soc.* .
- [162] Muñoz-Darias, T. *et al.* Regulation of black-hole accretion by a disk wind during a violent outburst of V404 Cygni. *Nature* **534**, 75–78 (2016).
- [163] Crenshaw, D. M., Kraemer, S. B. & George, I. M. Mass Loss from the Nuclei of Active Galaxies. *Annu. Rev. Astron. Astrophys.* **41**, 117–167 (2003).
- [164] Castro Segura, N. *et al.* A persistent ultraviolet outflow from an accreting neutron star binary transient. *Nature* **603**, 52–57 (2022).
- [165] Merloni, A., Heinz, S. & di Matteo, T. A Fundamental Plane of black hole activity. *Mon. Not. R. Astron. Soc.* **345**, 1057–1076 (2003).
- [166] Falcke, H., Körding, E. & Markoff, S. A scheme to unify low-power accreting black holes. Jet-dominated accretion flows and the radio/X-ray correlation. *Astron. Astrophys.* **414**, 895–903 (2004).
- [167] King, A. L. *et al.* Regulation of Black Hole Winds and Jets across the Mass Scale. *Astrophys. J.* **762**, 103 (2013).
- [168] Nomura, M. & Ohsuga, K. Line-driven disc wind model for ultrafast outflows in active galactic nuclei - scaling with luminosity. *Mon. Not. R. Astron. Soc.* **465**, 2873–2879 (2017).
- [169] Giustini, M. & Proga, D. A global view of the inner accretion and ejection flow around super massive black holes. Radiation-driven accretion disk winds in a physical context. *Astron. Astrophys.* **630**, A94 (2019).
- [170] Proga, D. & Kallman, T. R. On the Role of the Ultraviolet and X-Ray Radiation in Driving a Disk Wind in X-Ray Binaries. *Astrophys. J.* **565**, 455–470 (2002).
- [171] Tomaru, R., Done, C., Ohsuga, K., Odaka, H. & Takahashi, T. The thermal-radiative wind in the neutron star low-mass X-ray binary GX 13 + 1. *Mon. Not. R. Astron. Soc.* **497**, 4970–4980 (2020).
- [172] Mizumoto, M., Nomura, M., Done, C., Ohsuga, K. & Odaka, H. UV line-driven disc wind as the origin of UltraFast Outflows in AGN. *Mon. Not. R. Astron. Soc.* **503**, 1442–1458 (2021).
- [173] Laha, S. *et al.* Ionized outflows from active galactic nuclei as the essential elements of feedback. *Nature Astronomy* **5**, 13–24 (2021).
- [174] Begelman, M. C., McKee, C. F. & Shields, G. A. Compton heated winds and coronae above accretion disks. I Dynamics. *Astrophys. J.* **271**, 70–88 (1983).
- [175] Contopoulos, J. & Lovelace, R. V. E. Magnetically Driven Jets and Winds: Exact Solutions. *Astrophys. J.* **429**, 139 (1994).

- [176] Fukumura, K., Kazanas, D., Contopoulos, I. & Behar, E. Magnetohydrodynamic Accretion Disk Winds as X-ray Absorbers in Active Galactic Nuclei. *Astrophys. J.* **715**, 636–650 (2010).
- [177] Fukumura, K. & Tombesi, F. Constraining X-Ray Coronal Size with Transverse Motion of AGN Ultra-fast Outflows. *Astrophys. J. Lett.* **885**, L38 (2019).
- [178] Fukumura, K., Kazanas, D., Contopoulos, I. & Behar, E. Modeling High-velocity QSO Absorbers with Photoionized Magnetohydrodynamic Disk Winds. *Astrophys. J. Lett.* **723**, L228–L232 (2010).
- [179] Chakravorty, S. *et al.* Absorption lines from magnetically driven winds in X-ray binaries. *Astron. Astrophys.* **589**, A119 (2016).
- [180] Waters, T. & Proga, D. Magnetothermal disc winds in X-ray binaries: poloidal magnetic fields suppress thermal winds. *Mon. Not. R. Astron. Soc.* **481**, 2628–2645 (2018).
- [181] Tomaru, R., Done, C. & Mao, J. What powers the wind from the black hole accretion disc in GRO J1655-40? *MNRAS submitted*, arXiv:2204.08802 arXiv:2204.08802 (2022).
- [182] Fukumura, K. *et al.* Modeling Magnetic Disk Wind State Transitions in Black Hole X-Ray Binaries. *Astrophys. J.* **912**, 86 (2021).
- [183] Miller, J. M. *et al.* Powerful, Rotating Disk Winds from Stellar-mass Black Holes. *Astrophys. J.* **814**, 87 (2015).
- [184] Everett, J. E. Radiative Transfer and Acceleration in Magnetocentrifugal Winds. *Astrophys. J.* **631**, 689–706 (2005).
- [185] Ohsuga, K., Mineshige, S., Mori, M. & Kato, Y. Global Radiation-Magnetohydrodynamic Simulations of Black-Hole Accretion Flow and Outflow: Unified Model of Three States. *PASJ* **61**, L7–L11 (2009).
- [186] Luminari, A. *et al.* Speed limits for radiation driven SMBH winds. *arXiv e-prints* arXiv:2012.07877 (2020).
- [187] Proga, D. & Kallman, T. R. Dynamics of Line-driven Disk Winds in Active Galactic Nuclei. II. Effects of Disk Radiation. *Astrophys. J.* **616**, 688–695 (2004).
- [188] Matthews, J. H. *et al.* Stratified disc wind models for the AGN broad-line region: ultraviolet, optical, and X-ray properties. *Mon. Not. R. Astron. Soc.* **492**, 5540–5560 (2020).
- [189] Shakura, N. I. & Sunyaev, R. A. Reprint of 1973A&A....24..337S. Black holes in binary systems. Observational appearance. *Astron. Astrophys.* **500**, 33–51 (1973).
- [190] Shidatsu, M., Done, C. & Ueda, Y. An Optically Thick Disk Wind in GRO J1655-40? *Astrophys. J.* **823**, 159 (2016).
- [191] Reeves, J. N. *et al.* A New Relativistic Component of the Accretion Disk Wind in PDS 456. *Astrophys. J. Lett.* **854**, L8 (2018).
- [192] Boissay-Malaquin, R., Danehkar, A., Marshall, H. L. & Nowak, M. A. Relativistic Components of the Ultra-fast Outflow in the Quasar PDS 456 from Chandra/HETGS, NuSTAR, and XMM-Newton Observations. *Astrophys. J.* **873**, 29 (2019).
- [193] Begelman, M. C. & McKee, C. F. Compton heated winds and coronae above accretion disks. II. Radiativetransfer and observable consequences. *Astrophys. J.* **271**, 89–112 (1983).
- [194] Sim, S. A., Long, K. S., Miller, L. & Turner, T. J. Multidimensional modelling of X-ray spectra for AGN accretion disc outflows. *Mon. Not. R. Astron. Soc.* **388**, 611–624 (2008).
- [195] Motta, S. E., Kajava, J. J. E., Sánchez-Fernández, C., Giustini, M. & Kuulkers, E. The black hole binary V404 Cygni: a highly accreting obscured AGN analogue. *Mon. Not. R. Astron. Soc.* **468**, 981–993 (2017).
- [196] Giustini, M. & Proga, D. On the Diversity and Complexity of Absorption Line Profiles Produced by Outflows in Active Galactic Nuclei. *Astrophys. J.* **758**, 70 (2012).

- [197] Tombesi, F. *et al.* Wind from the black-hole accretion disk driving a molecular outflow in an active galaxy. *Nature* **519**, 436–438 (2015).
- [198] Gandhi, P. *et al.* An elevation of 0.1 light-seconds for the optical jet base in an accreting Galactic black hole system. *Nature Astronomy* **1**, 859–864 (2017).
- [199] Hitomi Collaboration *et al.* Atomic data and spectral modeling constraints from high-resolution X-ray observations of the Perseus cluster with Hitomi. *PASJ* **70**, 12 (2018).
- [200] Aharonian, F. A. *et al.* Hitomi Constraints on the 3.5 keV Line in the Perseus Galaxy Cluster. *Astrophys. J. Lett.* **837**, L15 (2017).
- [201] Gu, L. *et al.* Charge exchange in galaxy clusters. *Astron. Astrophys.* **611**, A26 (2018).
- [202] Mehdipour, M., Kaastra, J. S. & Kallman, T. Systematic comparison of photoionised plasma codes with application to spectroscopic studies of AGN in X-rays. *Astron. Astrophys.* **596**, A65 (2016).